Activated carbon from mustard stalk biomass: Synthesis, characterization and application in wastewater treatment

KALPANA PATIDAR and MANISH VASHISHTHA*

Department of Chemical Engineering, Malaviya National Institute of Technology, Jaipur 302017, Rajasthan India

Abstract: Present work is focused on the preparation of mustard stalk activated carbon (MSAC) using chemical activation with H_3PO_4 and exploring its properties for its use in dye removal from wastewater. Adsorption variable (dosage, contact time, and solution pH), pore structure, morphology, surface functional groups, equilibrium kinetics and isotherm study for the removal of methylene blue (MB) using MSAC were investigated. The present study showed that an adsorption dosage of 0.2 g L^{-1} and pH 8 can be considered as optimum for the MB removal. SEM result showed that pore of MSAC was larger than the pore of the mustard stalk (MS). BET surface area and total pore volume of MSAC were found as 510 m^2 g^{-1} and 0.33 cm^3 g^{-1}, respectively. Equilibrium adsorption data were examined by Langmuir and Freundlich isotherm models. Better correspondence to the Langmuir model with a maximum adsorption capacity of 212.76 mg g^{-1} (MB onto MSAC) was obtained. Dimensionless factor, R_L revealed favourable nature of the sorption in the MSAC–MB system. Adsorption rates were found to follow the pseudo-second-order kinetics with good correlation. These results show that the MSAC could be used as a renewable and economical alternative to commercial activated carbon in the removal of MB dye from wastewater.

Keywords: adsorption; isotherm; methylene blue; kinetics.

INTRODUCTION

Effluent from various process industries leads to significant pollution due to the transportation of aqueous dye solution into the water bodies and soil. Majority of dyes used in industries are of synthetic origin and are toxic in nature, among the synthetic dyes used in various industries. Methylene blue (MB) is a commonly used cationic dye (chemical name tetraethylthionine chloride, $C_{16}H_{18}ClN_3S$ and molecular weight is 319.85 g mol^{-1}) which finds application in the textile industry to color leather, wool, cotton, and also in paper coating.[1]

Toxicity of MB manifests itself in form of teratogenicity, mutagenicity, neuro-toxicity, nucleic acid damage, *etc*. Chronic exposure to MB dye leads to adverse health problems like vomiting, change in mental state or confusion, high pulse rate, jaundice, shock, burns injury of the eye, tissue necrosis, cyanosis, and limb paralysis, making it imperative to invent some efficient dye removal techniques from wastewater.[2] Also, MB and other dye laden wastewater adversely impact the aquatic ecosystem along with deteriorating the visual appeal of any water body by making it coloured and sometimes also leads to an obnoxious smell. Some important techniques used to treat dye-containing industrial wastewater (values in bracket indicate removal efficiency) includes biological (86 %), oxid-ation (90 %), ozonation (94.5 %), photochemical (99 %), adsorption (99 %), ion exchange (86.8 %), coagulation and flocculation (93.6 %), electrochemical (88.8 %), membrane technology (97.1 %) *etc*.[3,4] Some of these methods have disad-vantages like the formation of large quantities of hazardous by-products, often high energy-intensive, and high operating costs.[5] Among the above-listed methods adsorption process using activated carbon is far more effective for dye removal from effluent keeping the environmental perspective in view.

Activated carbon (AC) as the name suggests is a carbon-based material in form of solid black powder resembling powdered or granular charcoal. Its pecu-liar characteristics like its highly porous nature leading to the availability of large internal surface area coupled with its sufficiently high mechanical strength make it suitable for use as an effective adsorbent with widespread industrial applic-ations such as in gas purification, wastewater treatment (domestic and industrial), and as catalyst or catalyst supports.[6] Many textile industries widely use comer-cial AC for the treatment of wastewater carrying dyes in aqueous solution owing to its ability to treat dye laden wastewater in more concentrated forms.[7] The high cost of AC presents difficulty in its use on a large scale and consequently, the development of low-cost alternative adsorbents is needed as soon as possible and a lot of research is going on in this direction.

Coal and agricultural residues, rich in lignocellulosic content, are two major sources of the commercial-grade AC. Out of these sources, the agricultural wastes proved to be an economical bet for making AC due to two reasons: firstly, it helps in the saving of depleting fossil fuel (coal/coke) and secondly, it helps in the sustainable waste management by enormous agro residues generated. Some of the agricultural residues finding applications in making adsorbent include saw-dust[8], mustard husk[9,10], peanut shell[11], tobacco residues,[12] *etc*.

The physicochemical properties of AC are mainly governed by the technique of activation, activating agent, and the nature of precursor. Two available modes for the production of AC are physical and chemical activation. Chemical acti-vation is preferred over the physical method because of its less time consuming, requires low heating temperature, provides high specific surface area along with

well-controlled porosity.[13] Despite the various available chemical activation agents (like KOH, K_2CO_3, NaOH and Na_2CO_3), H_3PO_4 was found as a suitable reagent due to its low-cost and an environment-friendly dehydrating catalyst, which helps in the decomposition of the component present in MS at relatively low activation temperatures along with causing less corrosion to the activation equipment.[14]

The present work is focused on the development of an alternative, efficient, low-cost AC using mustard crop residue (MCR). The presence of glucosinolate content in MCR which is hazardous to animal health renders it unfit for consumption as fodder also thus making it imperative to convert it into other value-added product.[15] Mustard is one of the major oilseed crops grown globally in China, India, EU, and Canada as prominent producers, and its global annual production for 2019–20 is about 68.19 million metric tons per year.[16] India as a major mustard producer (annual production of 7.7 million metric tons per year) contributes 11.29 % to global production. Processing one ton of the mustard seed yields 1.85 tons of residue in form of mustard straw and husk.[17]

Not much research is reported on the utilization of mustard stalk (MS) as a renewable and economical source of the upgraded product as AC.[9,10] Thus to enhance the existing knowledge the present work is carried out by the adsorption of MB on MSAC from MS studied at different in adsorbent dosage, contact time, dye concentration, and pH. The obtained AC was characterized by proximate and ultimate analysis, BET surface area, SEM-EDX, TG and FTIR to explore its possibility of being used as a low-cost adsorbent for the removal of MB. Also, the isotherm and the kinetic models were applied to find out a better understanding of the adsorption process of MB on MSAC.

EXPERIMENTAL

Materials

MS for the preparation of AC was obtained from a village located close to the institute near Jaipur which is situated in Rajasthan, India (Variety, PM-21). For the experiment, analytical grade reagents used were: MB as adsorbate, H_3PO_4 as activation agent (99.99 wt.% purity), and HCl for washing (99.99 wt.% purity). All these solutions and reagents were purchased from Sigma–Aldrich. Double distilled water was used in the dilution and washing of samples.

Activated carbon preparation

The chemical activation method was followed by the preparation of AC using raw MS and H_3PO_4 as activating agent. The methodology for AC production used in the present work is depicted in Fig. 1.

The above methodology starts from MS being first washed with hot distilled water to remove the attached impurities (dust, *etc*.) and then dried in a hot air oven at 105 °C for 24 h followed by crushing, grinding, and sieving to obtain particles of 60 mesh sizes. Powdered MS is then subjected to carbonization by putting it in a furnace for 1 h, maintained at 550 °C under an inert atmosphere to obtain MS char. 30 g of this char was impregnated at 80 °C for 6

h with 250 cm^3 solutions containing the activating agent (H$_3$PO$_4$). The mixture was dehydrated overnight in an oven at 105±1 °C for 24 h. The dried samples were further thermally treated at a temperature of 768 °C in a muffle furnace, in the oxygen-deficient atmosphere for 60 min, in order to obtain MSAC. The optimum conditions for activation were reported in our previous work.[18] MSAC sample obtained was thoroughly washed using hot and cold distilled water to remove any excess H$_3$PO$_4$ until neutral pH was obtained. After thorough washing, the samples were dried overnight in a hot air oven at 105 °C, and thereafter weighed and packed for future characterization.
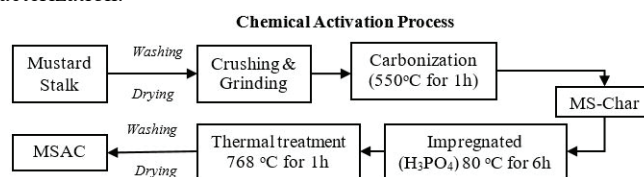
Chemical Activation Process

Fig. 1. MSAC production methodology.

Characterization of adsorbent

The surface morphology and the elemental analysis of MS and MSAC were done using scanning electron microscopy (SEM) with energy dispersive X-ray analysis (EDX, Nova Nano FE-SEM 450, FE). The functional groups present in the sample were characterized by Fourier transform infrared (FTIR, FT-IR Spectrum 2, Perkin Elmer) with a working range of 4000 to 500 cm^{-1}. Thermogravimetric (TG, SII 6300 EXSTAR, India) analysis was carried out by heating a 10 mg MS sample in a purge of nitrogen (flow rate 200 ml min^{-1}), and a temperature range from ambient to 727 °C at 20 °C min^{-1} heating rate. The ASTM D3174-73 standard was adopted for the ash content determination and the nitrogen adsorption/desorption experiments were conducted by Quantachrome Autosorb analyzer (using N$_2$ at 77 K). The total pore volume was performed by nitrogen adsorption at p/p_o = 0.98.

Equilibrium and isotherm studies

The experiments for adsorption of MB on MSAC were studied at different adsorbent dosage, contact time, dye concentration, and pH. Changes in any of these parameters will affect the rate of adsorption. To achieve the desired rate of removal, the optimum adsorption conditions should be determined. The study of adsorption isotherm and the adsorption kinetics is done. The runs and conditions at which the adsorption experiments were conducted are presented in Table I.

The fixed amount of adsorbent (0.2 g L^{-1}) MSAC in our case was mixed with MB dye solutions of different initial concentrations, ranging from 10-50 mg L^{-1} in 250 mL conical flasks, for obtaining the adsorption equilibrium. The mixture was mixed at 160 rpm for 180 min. Once the agitation is completed, the dye solution was subjected to centrifugation for 15 min at a speed of 2800 rpm, due to which the char particles settled at the bottom of the tube. UV-Vis spectrophotometer (Evolution 220, Thermo Fisher Scientific, USA) at a wavelength of 664 nm was employed to determine the concentration of MB solution. The removal percentage (R) of the dye (MB) by the MSAC (adsorbents), the adsorption capacity of MB at equilibrium, q_e / mg g^{-1}, and the amount of adsorption at time t, min, q_t / mg g^{-1}, was calculated using Eqs. (1)–(3) respectively:

$$R = 100\frac{C_o - C_e}{C_o} \qquad (1)$$

$$q_e = \frac{(C_o - C_e)}{W} V \tag{2}$$

$$q_t = \frac{(C_o - C_t)}{W} V \tag{3}$$

here, C_o (initial state), C_t (any time), and C_e (equilibrium state) represents the MB concentrations of dye solution in mg L^{-1} respectively; V / L is the dye solution volume of the dye and W / g is the mass of dry AC (adsorbent) used.

TABLE I. Runs and conditions of adsorption experiment

Experimental item	MSAC content, g L^{-1}	Concentrations of dyes, mg L^{-1}	Sampling time, min	Temperature °C	Vibration rate, rpm
Effect of dosage	0.05 to 0.3 (0.05, 0.1, 0.15, 0.2, 0.25, 0.3)	30	180	30	160
Effect of concentration with time	0.2	10 to 50 (10, 20, 30, 40, 50)	30 to 180 (30, 60, 90, 120, 180)	30	160
Effect of pH	0.2	30	180	30	160
Adsorption isotherms	0.2	10 to 50 (10, 20, 30, 40, 50)	180	30	160
Adsorption kinetics	0.2	10 to 50 (10, 20, 30, 40, 50)	30 to 180 (30, 60, 90, 120, 180)	30	160

RESULTS AND DISCUSSION

Characterization of sample

TG analysis. TG analysis (Fig. 2) was done to study the general decomposition behaviour of MS before the activation. The TGA profiles depict the trend of mass loss occurring in the sample with time when heated in the temperature range of 30-200 °C, this weight loss is due to the dehydration of the MS sample.[19] The loss of unbound moisture resulted in an 11.08 % decrease in weight in the above temperature range. This value bears a close resemblance to the moisture percentage of the MS (Table II).
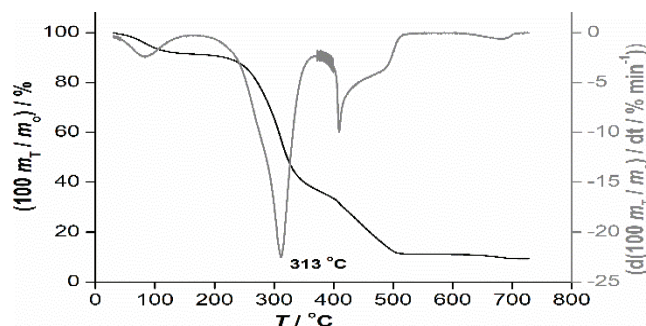

Fig. 2. TG analysis of MS at 20 °C min^{-1}.

The maximum weight loss occurred between the 200–467 °C range, which is a result of thermal decompositions of hemicellulose, cellulose and partial decomposition of lignin present in the biomass sample.[20] In this range, the mass loss is about 74 %. The main peak in the DTG curve is observed at ~313 °C due to the thermal decomposition of the above components present in MS. As the temperature is increased beyond 500 °C weight loss that is not very significant takes place due to no further breakdown of lignocellulosic material. Weight loss at the final temperature of 727 °C is 90.25 %. Thus, from the above observations, it can be inferred that the temperatures beyond 550 °C are more suitable for the conducting of activation, since the sample shows insignificant decomposition.

SEM-EDX analysis. The element-wise composition of raw MS and MSAC samples are given in Table II from which it is clear that the use of H_3PO_4, as an activating agent has a significant influence on the production of AC with the sufficiently high carbon content (68.64 %). The carbon percentage of the MSAC samples shows a marked increase as compared to the raw MS (53.68 %) after the activation process; however, oxygen, hydrogen, and nitrogen contents exhibit the opposite trend, as expected. Due to the high temperature carbonization and the activation process, the MS undergoes decomposition which occurs together with the expulsion of volatile compounds (*viz.*, oxygen, hydrogen, nitrogen), contained by the formed MSAC, thus making it carbon-rich. Also, the chemical activation of MS using H_3PO_4 selectively strips H and O away from it.

The morphology of MS is shown in Fig. 3a from which it can be seen that the basic structure of MS comprises longitudinal fibres and it seems that the pores are preserved in the fibrous cellular structure. However, after the chemical activation of MS to obtain MSAC, as seen in Fig. 3b, a more randomized pore/ /cavities distribution is obtained, which can be attributed to the modification of cellular structure by the acid activation agent. Rich cavities surface of MSAC will provide favourable adsorptive property towards MB dye molecules.

TABLE II. Ultimate, proximate and BET analysis of MS and MSAC

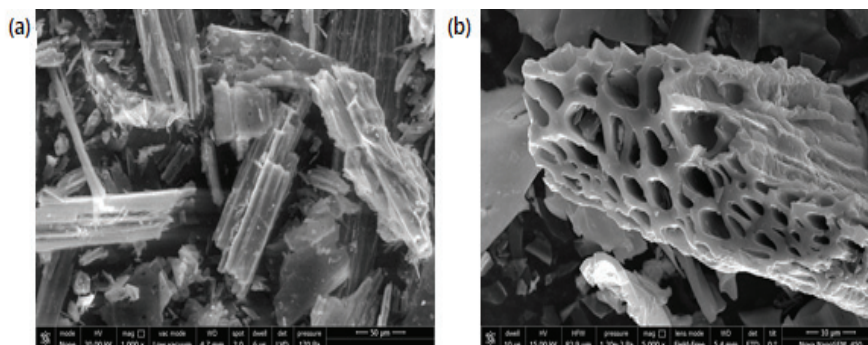| Proximate analysis	Content, wt.%		Surface property	Content, wt.%	
	MS	MSAC		MS	MSAC
Moisture	9.58	4.32	Bulk density, kg m^{-3}	86	503.23
Volatile material	71.92	15.32	Average pore diameter, nm	–	2.64
Ash	4.41	9.59	BET surface area, m^2 g^{-1}	95	510
Fixed carbon	14.09	70.77	Total pore volume, cm^3 g^{-1}	0.081	0.33
			Mesoporous volume, cm^3 g^{-1}	0.06	0.17
Ultimate analysis					
C	53.68	68.64			
H	4.04	1.23			
N	2.90	2.97			
O	43.45	23.97			
S	0.08	0.40			

Fig. 3. Morphology of: (a) MS and (b) MSAC prepared with H_3PO_4 activation.

FTIR and BET surface area analysis. The sample surface functional groups are detected using FTIR spectroscopy. The FTIR spectra of the MS, MSAC before and after the MB adsorption as shown in Fig. 4a and b, respectively, and they show a variation of peaks with intensity and position arising out of the vibrational variations of the surface functional groups. The adsorption peak at 3500––3250 cm^{-1} (due to stretching vibration of O–H) was of low intensity in MSAC. The peak intensity reduces due to a corresponding reduction in H-bonding, happening as a result of a reaction between activating agent which in the present case is H_3PO_4 (acting as a dehydrating agent) and MS.[21]
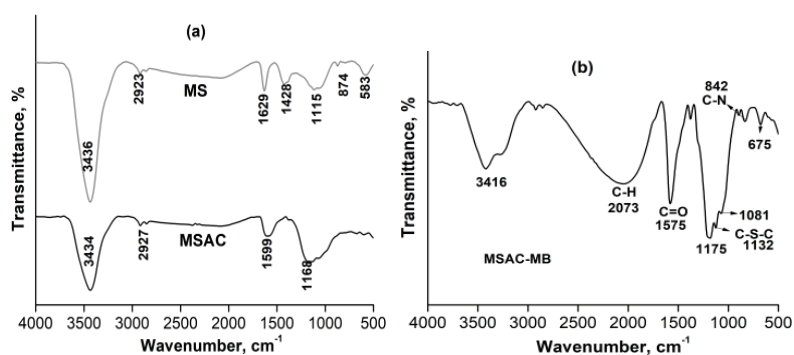

Fig. 4. FTIR spectra of: a) MS and MSAC and b) MSAC-MB.

The peaks corresponding to the bandwidth of 2902–2939 cm^{-1}, arising due to the asymmetric C–H stretching vibration of alkanes and alkyl groups, are more prominent for the raw MS *vis a vis* MSAC. The underlying phenomena behind this observation is a large scale hydrogen removal during the activation process. The ultimate analysis also depicts this trend of reduction in hydrogen and oxygen content of MSAC (Table II).

The band at 1600–1500 cm^{-1} (C=C band of the aromatic rings) shows the aromatization of adsorbent.[22] After activation with H_3PO_4, a peak at around

1168 cm^{-1} appear in the FTIR spectrum of MSAC, which corresponds to P–O–C vibrational variations of aliphatic phosphates groups. 1000–1250 cm^{-1} (stretching vibration of C–O and/or C–O–C in acids, phenols, alcohols, ethers, and/or esters groups).[23] The band about 914 and 756–697 cm^{-1} shows C–H out-of-plane bending in an aromatic ring. The peaks at 3434, 2927, 1599 and 1168 cm^{-1} are shifted to 3416, 2905, 1575 and 1132 cm^{-1}, respectively (Fig. 4b). This shift in the absorption peak suggested the interactions of dye molecules with the functional groups of MSAC.

The BET surface area, total pore volume, and mesoporous volume of MSAC were calculated as 510 m^2 g^{-1}, 0.33 and 0.171 cm^3 g^{-1} respectively (Table II). The increases in the pore volumes and average pore radius after activation is a result of macropores deformation resulting in their transformation into mesoporous due to the H$_3$PO$_4$ effect.

Effect of an operational parameter on MB adsorption

Effect of adsorbent (MSAC) dosage. The adsorption of MB on MSAC was studied at an initial concentration of 30 mg L^{-1} by varying the quantity of adsorbent (0.05, 0.1, 0.15, 0.2, 0.25 and 0.3 g L^{-1}) at 30 °C temperature and pH 8. The experiments were carried out at a contact time of 180 min. As shown in Fig. 5a, the removal of MB shows an increasing trend up to 0.2 g, and beyond that it remains unaltered. At the equilibrium time, the removal shows an increase from 31.42 to 98.52 % with an increment in MSAC dosage from 0.05 to 0.2 g. The increased removal of MB is a result of an enhanced adsorbent surface area and the availability of more adsorption sites.

Effect of the initial concentration of MB on contact time. The effect of initial MB concentration in a range between 10–50 mg L^{-1}, at a fixed adsorbent dosage of 0.2 g at 30 °C temperature and a speed of 160 rpm, was studied and its effect on the adsorption of MB onto MSAC is shown in Fig. 5b. The plots of Fig. 5b can be bifurcated into three different regions:

– Region 1: corresponding to rapid adsorption during the first 30 min.

– Region 2: corresponding to the gradual equilibrium till the equilibrium state for each concentration is reached.

– Region 3: depicting the equilibrium state.

The results show that with an increase in initial MB concentration, a corresponding increase in the adsorption of MB on MSAC is observed. The MB adsorption increased from 52.63 to 198.45 mg g^{-1} at equilibrium, when the initial MB concentration is increased from 10 to 50 mg L^{-1}. Furthermore about this change in MB concentration, the equilibrium removal of MB exhibits a decrease from 99.65 to 79.38 %. This can be attributed to the fact that when the initial concentration increases, the mass transfer driving force increases, resulting in

higher MB adsorption. The comparable trends were obtained in similar studies of adsorption of MB on tea waste.[24]
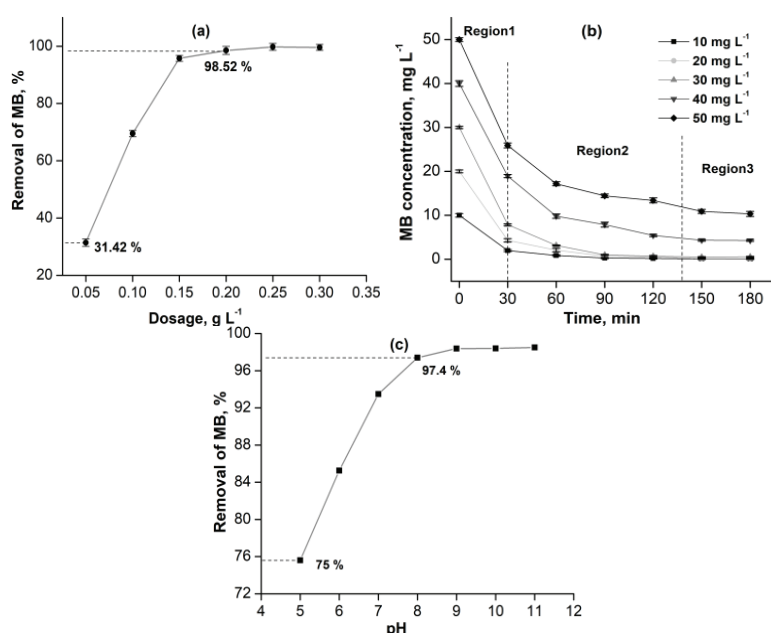

Fig. 5. Effect of: a) MSAC dosage on removal of MB (C_o = 30 mg L^{-1}, pH 8.0); b) contact time and initial concentration on MB adsorption (adsorbent dose = 0.2 g L^{-1}, pH 8.0); c) effect of pH on MB removal (C_o = 30 mg L^{-1}, adsorbent dose = 0.2 g L^{-1}); contact time = 180 min, temperature = 30 °C.

Also, it is evident from Fig. 5b that at an initial concentration ranging between 10 and 30 mg L^{-1}, the adsorption equilibrium is achieved in less than 60 min. However, when the initial MB concentration is increased to 40–50 mg L^{-1}, the corresponding time achieves the equilibrium becomes 150 min. However, the experimentation was carried at 180 min in order to ensure the attainment of the full equilibrium. The dye adsorption follows a sequential process in which at first instance the dye molecules has encounter the boundary layer effect, followed by the diffuse boundary layer film to the adsorbent surface, and finally the diffusion into the porous structure of the adsorbent.[25] Hence, higher initial concentrations of MB solutions will take a relatively longer contact time to attain the equilibrium due to the presence of a higher number of dye molecules.

Effect of pH. pH plays a prominent role in governing the adsorbent capacity in wastewater treatment processes. Fig. 5c presents the effect of pH on MB removal by MSAC. As the pH is changed from 5 to 8 the removal percentage of MB increased from 75 to 97.4 %.

The removal of MB increases rapidly up to pH 8 and then the equilibrium is reached. The maximum percentage removal of about 98.40 % is obtained in a pH range of 9–11. This variation is observed since the adsorption depends on the adsorbent surface and structure of MB.[25] Acidic medium promotes the protonation of MB, however as the pH increases the dye becomes more and more deprotonated. The low MB removal (indicated by dark blue colour) in the lower pH range can be due to the probable development of the positive charge at the MSAC surface, which inhibits MB removal from the dye.[10] However, beyond pH 8, when the medium becomes basic in nature, there seems to be a significant change in polarity, as MB removal increases (solution becomes light blue) monotonically with pH. Thus, a low pH (<6) is the unfavourable use of MSAC. As the initial pH (natural pH 6) of MB solution decreases, the number of negatively charged adsorbent sites decrease and the positively charged sites increases, which does not favour the adsorption of positively charged MB cations due to electrostatic repulsion.[26]

Adsorption isotherm

Distributions of the adsorbed molecules between the liquid and solid phases, when the adsorption process attains an equilibrium state, are shown by the adsorption isotherms. For the design purposes, the suitable models are needed which can be developed by fitting isotherm data into different isotherm models.[26] Various models are proposed in the literature to explain the data about the adsorption isotherms, among which Langmuir and Freundlich are the most commonly used models. In the present work, both models were applied to understand the relationship between the amount of dye adsorbed and its equilibrium concentration.[27]

The linear isotherm equations are as following:

Langmuir:

$$\frac{C_e}{q_e} = \frac{1}{Q_m K} + \frac{C_e}{Q_m} \tag{4}$$

$$R_L = \frac{1}{\left(1 + K C_o\right)} \tag{5}$$

Freundlich:

$$\ln q_e = \ln K_f + \frac{1}{n} \ln C_e \tag{6}$$

where is q_e / mg g^{-1}: the amount of adsorbed at the equilibrium time, C_o / mg L^{-1}: the initial solute concentration, C_e / mg L^{-1}: the equilibrium concentration of adsorbate in solution, Q_m / mg g^{-1}: the maximum adsorption capacity corresponding to the complete monolayer coverage, K / L mg^{-1}: the Langmuir constant

related to the energy of the adsorption, K_f, and $1/n$: the empirical constants dependent on the nature of adsorbent and adsorbate. The R_L value implies the favourable adsorption process at a temperature range from 30–50 °C.

Both K_f and $1/n$ are important in selecting an adsorbent as a separating medium, in which K_f / mg g^{-1} is the over-all adsorption capacity and $1/n$ is the heterogeneity factor. The adsorption will be chemical if the $n < 1$, linear if the $n = 1$, and if the $n > 1$ the adsorption will be a physical process.

The adsorption isotherms fitting the two models were shown in Fig. 6. From the values of constants for both isotherm were computed from the slope and the intercept of the linear plot, which and listed in Table III. The R^2 value obtained from the Langmuir isotherm (Fig. 6a) was higher than that obtained from the Freundlich isotherm (Fig. 6b). This evidence suggested that better fitting is achieved by the Langmuir isotherm. The maximum capacity obtained by Langmuir isotherm is 212.76 mg g^{-1}, showing the monolayer coverage and uniform surface adsorption on MSAC. The R_L value implies the adsorption to be unfavourable ($R_L > 1$), linear ($R_L = 1$), favorable ($0 < R_L < 1$) or irreversible ($R_L = 0$).[28] In the present work value of R_L was found to be 0.0035 and thus it confirms that the prepared AC, MSAC is favourable for the adsorption of MB dye under the conditions used in this study. The values of n higher than unity shows that the adsorption of MB on MSAC is a physical process.
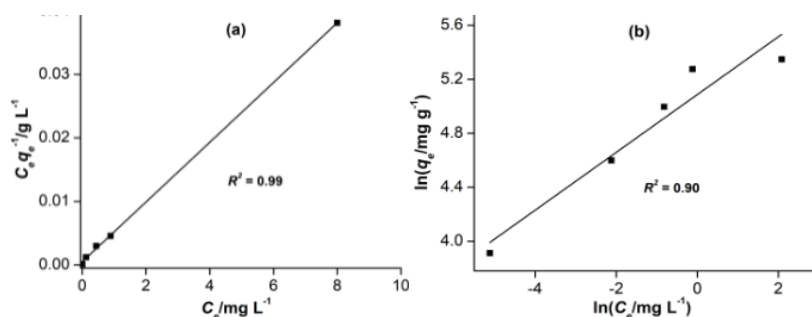

Fig.6. Linearized: a) Langmuir isotherm, b) Freundlich isotherm for MB adsorption by MSAC (pH 8, dosage = 0.2 g L^{-1}, $T = 30$ °C).

TABLE III. Langmuir, Freundlich adsorption isotherm constant for MB dye on MSAC

Langmuir isotherm			Freundlich isotherm		
Q_m / mg g^{-1}	K / L mg^{-1}	R^2	$1/n$	K_f / mg g^{-1} L mg$^{-1/n}$	R^2
212.76	9.179	0.999	0.2142	160.77	0.90

Adsorption kinetics

The experimentally obtained kinetic adsorption data were subjected to the pseudo-first-order kinetic and the pseudo-second-order kinetic model.[27]

Pseudo-first-order kinetic:

$$\log(q_e - q_t) = \log q_e - \frac{k_1}{2.303}t \qquad (7)$$

Pseudo-second-order kinetic:

$$\frac{t}{q_t} = \frac{1}{k_2 q_e^2} + \frac{1}{q_e}t \qquad (8)$$

Where is k_1 / 1 min^{-1}: rate constant of first order adsorption, q_e / mg g^{-1}: the amount of solute adsorbed at equilibrium, q_t / mg g^{-1}: the amount of solute adsorbed on the surface of the sorbent at any time, min.

Fig. 7a and b) shows the pseudo-first-order kinetic and pseudo-second-order kinetic model was fitted with the adsorption kinetic data of MB on MSAC. The slope and the intercept were used to calculate the model constant kinetic parameter, and were given with the correlation coefficients (R^2) in Table IV. The correlation coefficient, R^2 for the pseudo-second-order adsorption model has a high value is 0.99, and also its calculated equilibrium adsorption capacity, $q_{e,cal}$ is consistent with the experimental data. These facts suggest that the pseudo-second-order adsorption mechanism is predominant and that the overall rate of the dye adsorption process is chemisorption controlled.
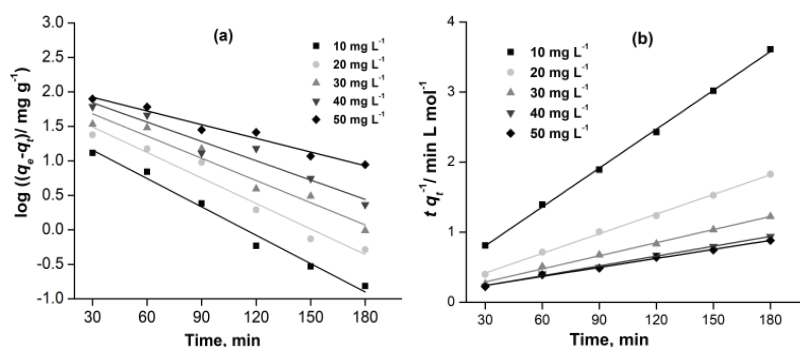

Fig. 7. a) Pseudo-first-order kinetics and b) pseudo-second-order kinetics for MB adsorption by MSAC (pH 8, dosage = 0.2 g L^{-1}, T = 30 °C).

TABLE IV. Pseudo-first- and pseudo-second-order kinetics constant for MB dye on MSAC

C_o / mg L^{-1}	Pseudo-first-order kinetic model				Pseudo-second-order kinetic model		
	$q_{e,exp}$ mg g^{-1}	$q_{e,cal}$ mg g^{-1}	k_1 L min^{-1}	R^2	$q_{e,cal}$ mg g^{-1}	k_2 g mg^{-1} min^{-1}	R^2
10	52.63	36.78	0.031	0.98	54.11	0.00135	1
20	105.1	72.6	0.028	0.94	107.06	0.00063	1
30	156.82	100.83	0.024	0.94	160.51	0.00037	1
40	208.65	132.53	0.021	0.93	213.67	0.00022	1
50	228.33	134.89	0.015	0.96	233.64	0.00016	0.997

Table V presents the adsorption capacities and BET surface area of the various biomass-based AC removal of dye. The surface area of MSAC is $510 \text{ m}^2 \text{ g}^{-1}$, is about a fivefold increase in surface area as compared to raw MS; also, the surface area of MSAC is comparable to the AC produced from other biomass-based AC, prepared using the same chemical activation route as shown in Table V. It can be inferred that the adsorption capacity of MSAC is quite comparable or even greater than that of some adsorbents reported in references.

TABLE V. Adsorption capacity and BET surface area of other biomass-based AC prepared using H_3PO_4

Material	Dye	Activating agent	BET surface area, $\text{m}^2 \text{ g}^{-1}$	Adsorption capacity, mg g^{-1}	Reference
MSAC	Methylene blue	H_3PO_4	510	212.76	Present study
Yellow mombin fruit stones	Dianix® royal blue CC	H_3PO_4	551	147.47	14
Tea waste	Methylene blue	–	–	85.16	24
Shrimp shell	Methylene blue	H_3PO_4	506	828	27

Adsorption mechanism for MB

Based on the above results, the activation process and the adsorption mechanism can be represented by Fig. 8. The prepared MSAC is rich in the hydroxyl group on their surface, which is also testified by the FTIR spectra.
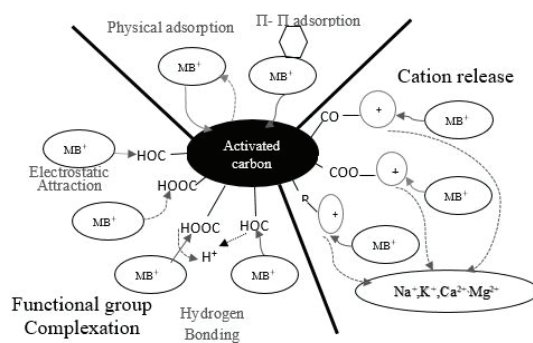

Fig. 8. Mechanism for MB adsorption onto MSAC.

The adsorption of MB by AC can be explained in terms of three major mechanisms: *i*) the electron-donor mechanism, *ii*) the π–π interaction and *iii*) the effect of solvent. An electron-donor mechanism is based on sharing of the electrons which occurs between the MSAC (adsorbent) and MB (adsorbate), the aromatic ring of MB acts as an electron acceptor and the surface functional groups, present on MSAC, act as donor.[29] The π–π interaction occurs due to the charge transfer happening between the π electrons of the benzene ring and the MSAC surface. The third mechanism, namely solvent effect, means that the adsorbed

water molecules have quite a high possibility of being attracted to the surface –O– groups, which leads to the formation of H– bonds between them. However, this interaction inhibits the adsorption capacity, as it may cover active sites on the MSAC.[30]

CONCLUSIONS

The present study shows that MSAC is a good low-cost adsorbent, derived from the agricultural waste. It is well suited for the removal of MB from aqueous solution. The dye adsorption is affected by various factors like adsorbent dosage, contact time, pH, and the concentration of dye. The equilibrium is practically achieved in less than 180 min. The characterization result showed that the BET surface area and the total pores volume of the MSAC is 510 m^2 g^{-1} and 0.32 cm^3 g^{-1}, respectively. Also, it has high carbon content (68.84 %) along with a highly porous surface with cracks, channels, and large holes. The Langmuir and the Freundlich adsorption isotherms are used for the analysis of equilibrium data. The Langmuir model better explains the data. The maximum adsorption capacity obtained was 212.76 mg g^{-1}, with the monolayer coverage of MB molecules at the outer surface of MSAC. The value of R_L was found to be 0.0035 and confirmed that the prepared MSAC is favourable for the removal of MB dye from wastewater. The pseudo-second-order kinetics model is best fitted for MB adsorption onto MSAC. These results show that the MSAC could be applied as a low-cost alternative to the commercial AC in the removal of MB dye from wastewater.

ИЗВОД

АКТИВНИ УГАЉ ОД БИОМАСЕ СТАБЉИКЕ СЛАЧИЦЕ (*Sinapsis alba*) – СИНТЕЗА , КАРАКТЕРИЗАЦИЈА И ПРИМЕНА У ПРЕЧИШЋАВАЊУ ОТПАДНИХ ВОДА

KALPANA PATIDAR и MANISH VASHISHTHA

Department of Chemical Engineering, Malaviya National Institute of Technology, Jaipur 302017, Rajasthan India

Овај рад је фокиусиран на припрему активног угља од стабљика биљке *Sinapsis alba* (MSAC), добијеног хемијском активацијом H$_3$PO$_4$, као и испитивањем његове примене у уклањању боја из отпадних вода. Адсорпциони параметри (доза адсорбента, контактно време и pH раствора адсорбата), структура пора, морфологија, површинске функционалне групе, равнотежна кинетика и студија изотерми за уклањање метилен плавог (MB) коришћењем MSAC су такође испитивани. Приказани резултати показују да се доза адсорбента од 0,2 g L^{-1} и pH 8 могу сматрати оптималним за уклањање MB. SEM резултати указују да су поре MSAC веће од пора немодификоване биомасе (MS). Специфична површина добијена BET техником као и укупна запремина пора MSAC износе 510 m^2 g^{-1} и 0,33 cm^3 g^{-1}, редом. Равнотежни адсорпциони подаци корелисани су применом Lang-

muir и Freundlich модела. Боље слагање експерименталних података добијено је применом Langmuir модела са максималним адсорпционим капацитетом od 212,76 mg g^{-1} (MB на MSAC). Бездимензиони фактор, R_L, указује на повољне услове као и природу сорпционог MSAC–MB система. Адсорпциона брзина најбоље је описана кинетиком псеудо-другог реда, што се може уочити из корелационих резултата. Добијени резултати показујy се се адсорбент MSAC може користити у уклањању MB, као обновљива и економски исплатива алтернатива постојећим комерцијалним адосрбентима на бази активног угља.

REFERENCES

1. I. Bazin, A. Ibn Hadj Hassine, Y. Haj Hamouda, W. Mnif, A. Bartegi, M. Lopez-Ferber, M. De Waard, C. Gonzalez, *Ecotoxicol. Environ. Saf.* **85** (2012) 131 (http://dx.doi.org/10.1016/j.ecoenv.2012.08.003)
2. L. Liu, D. He, F. Pan, R. Huang, H. Lin, X. Zhang, *Chemosphere* **238** (2020) (http://dx.doi.org/10.1016/j.chemosphere.2019.124671)
3. A. H. Jawad, M. Bardhan, A. Islam, A. Islam, S. S. A. Syed-Hassan, S. N. Surip, *Surfaces Interfaces* (2020) 100688 (http://dx.doi.org/10.1016/j.surfin.2020.100688)
4. V. Katheresan, J. Kansedo, S. Y. Lau, *J. Environ. Chem. Eng.* **6** (2018) 4676 (http://dx.doi.org/10.1016/j.jece.2018.06.060)
5. M. Rafatullah, O. Sulaiman, R. Hashim, A. Ahmad, *J. Hazard. Mater.* **177** (2010) 70 (http://dx.doi.org/10.1016/j.jhazmat.2009.12.047)
6. B. Hu, Y. Ai, J. Jin, T. Hayat, A. Alsaedi, L. Zhuang, X. Wang, *Biochar* **2** (2020) 47 (http://dx.doi.org/10.1007/s42773-020-00044-4)
7. W. Xing, X., Jiang, W., Li, S., Zhang, X. and Wang, *Waste Manage.* **89** (2019) 64 (http://dx.doi.org/https://doi.org/10.1016/j.wasman.2019.04.002)
8. A. Kumar, H. Gupta, *Environ. Technol. Innov.* **20** (2020) (http://dx.doi.org/10.1016/j.eti.2020.101080)
9. S. Charola, H. Patel, S. Chandna, S. Maiti, *J. Clean. Prod.* **223** (2019) 969 (http://dx.doi.org/10.1016/j.jclepro.2019.03.169)
10. R. K. Gautam, A. Mudhoo, M. C. Chattopadhyaya, *J. Environ. Chem. Eng.* **1** (2013) 1283–1291 (http://dx.doi.org/10.1016/j.jece.2013.09.021)
11. D. Garg, C. B. Majumder, S. Kumar, B. Sarkar, *J. Environ. Chem. Eng.* **7** (2019) (http://dx.doi.org/10.1016/j.jece.2019.103365)
12. S. Archin, S. H. Sharifi, G. Asadpour, *J. Clean. Prod.* **239** (2019) (http://dx.doi.org/10.1016/j.jclepro.2019.118136)
13. Y. Gao, Q. Yue, B. Gao, A. Li, *Sci. Total Environ.* **746** (2020) 141094 (http://dx.doi.org/10.1016/j.scitotenv.2020.141094)
14. M. J. P. Brito, C. M. Veloso, L. S. Santos, R. C. F. Bonomo, R. da C. I. Fontan, *Powder Technol.* **339** (2018) 334 (http://dx.doi.org/10.1016/j.powtec.2018.08.017)
15. R. T. Zrybko, C.L., Fukuda, E.K. and Rosen, *J. Chromatogr. A* **767** (1997) 43–52 (http://dx.doi.org/https://doi.org/10.1016/S0021-9673(96)01068-0)
16. Statista, https://www.statista.com/statistics/263930/worldwide-production-of-rapeseed-by- country (visited October 25, 2020)
17. T. C. Purohit, P., Tripathi, A.K. and Kandpal, *Energy* **31** (2006) 1321 (http://dx.doi.org/10.1016/j.energy.2005.06.004)
18. K. Patidar, M. Vashishtha, *Water Air Soil Pollut* **231** (2020) 526 (https://doi.org/10.1007/s11270-020-04893-4)

19. S. Maiti, S. Purakayastha, B. Ghosh, *Fuel* **86** (2007) 1513
(http://dx.doi.org/10.1016/j.fuel.2006.11.016)
20. D. Vamvuka, E. Kakaras, E. Kastanaki, P. Grammelis, *Fuel* **82** (2003) 1949
(http://dx.doi.org/10.1016/S0016-2361(03)00153-4)
21. A. Kumar, H. M. Jena, *Results Phys.* **6** (2016) 651
(http://dx.doi.org/10.1016/j.rinp.2016.09.012)
22. S. J. C. E. J. Prahas, D. Kartika, Y. Indraswati, N. Ismadji, *Chem. Eng. J.* **140** (2008) 32
(http://dx.doi.org/https://doi.org/10.1016/j.cej.2007.08.032)
23. Y. Sun, H. Li, G. Li, B. Gao, Q. Yue, X. Li, *Bioresour. Technol.* **217** (2016) 239
(http://dx.doi.org/10.1016/j.biortech.2016.03.047)
24. M. T. Uddin, M. A. Islam, S. Mahmud, M. Rukanuzzaman, *J. Hazard. Mater.* **164**
(2009) 53 (http://dx.doi.org/10.1016/j.jhazmat.2008.07.131)
25. S. Senthilkumaar, P. R. Varadarajan, K. Porkodi, C. V. Subbhuraam, *J. Colloid
Interface Sci.* **284** (2005) 78 (http://dx.doi.org/10.1016/j.jcis.2004.09.027)
26. K. Aisan, H. Z. Mousavi, R. Alimorad, H. Shirkhanloo, *J. Serbian Chem. Soc.* **83**
(2018) 651 (http://dx.doi.org/10.2298/JSC170827112K)
27. L. Liu, X. He, C. Yu, X. Bai, Y. Ye, L. Wang, B. Zhang, *Powder Technol.* **326** (2018)
181 (http://dx.doi.org/https://doi.org/10.1016/j.powtec.2017.12.034)
28. K. C. Bedin, A. C. Martins, A. L. Cazetta, O. Pezoti, V. C. Almeida, *Chem. Eng. J.* **286**
(2016) 476 (http://dx.doi.org/10.1016/j.cej.2015.10.099)
29. Y. Tang, Y. Zhao, T. Lin, Y. Li, R. Zhou, Y. Peng, *J. Environ. Chem. Eng.* **7** (2019)
(http://dx.doi.org/10.1016/j.jece.2019.103398)
30. S. Fan, Y. Wang, Z. Wang, J. Tang, J. Tang, X. Li, *J. Environ. Chem. Eng.* **5** (2017)
601 (http://dx.doi.org/10.1016/j.jece.2016.12.019).